An alternative TLM method for steady-state convection-diffusion

Alan Kennedy[1,*,†] and William J. O'Connor[2]

[1]*School of Mechanical and Manufacturing Engineering, Dublin City University, Glasnevin, Dublin 9, IRELAND*
[2]*School of Electrical, Electronic and Mechanical Engineering, University College Dublin, Belfield, Dublin 4, Ireland*

SUMMARY

Recent papers have introduced a novel and efficient scheme, based on the Transmission Line Modelling (TLM) method, for solving one-dimensional steady-state convection-diffusion problems. This paper introduces an alternative method. It presents results obtained using both techniques which suggest that the new scheme outlined in this paper is the more accurate and efficient of the two.

INTRODUCTION

The convection-diffusion equation (CDE) describes physical processes in the areas of pollution transport, biochemistry, semiconductor behaviour, heat transfer, and fluid dynamics [1-3]. Recent papers have presented a novel Transmission Line Modelling (TLM) scheme, referred to here as the "varied impedance" (VI) method, which can solve the steady-state convection-diffusion equation in one dimension accurately and efficiently [4, 5]. The method is particularly efficient when the convection term dominates, a situation in which most traditional schemes have difficulty producing accurate results [1-3, 6].

The VI scheme, summarised below, is based on the correspondence, under steady-state conditions, between the equation for the voltage along a transmission line (TL) (for example, a pair of parallel conductors) and the convection-diffusion equation. Lossy TLM is a straightforward scheme, originally developed to solve diffusion equations [7, 8], which can be used to model the voltage along such a TL. It has been extended to model two- and three-dimensional diffusion problems by using a network of interconnected TLs [7, 9]. Although TLM usually models in the time-domain, steady-state solutions can be calculated directly [5]. There is a rigorous procedure, described fully elsewhere [4, 5], for determining the parameters of the TLM model from given coefficients of the CDE to be solved.

The novel method introduced here, referred to as the "convection line" (CL) scheme, essentially models two connected transmission lines, one that exhibits diffusion, and one that exhibits

[**]Correspondence to: Alan Kennedy, School of Mechanical and Manufacturing Engineering, Dublin City University, Glasnevin, Dublin 9, IRELAND
[†]E-mail: alan.kennedy@dcu.ie

convection. While there is no clear mathematical or physical basis for doing this, it will be shown below that the result is an efficient, accurate, and easily implemented technique for solving the steady-state CDE.

THE VARIED IMPEDANCE SCHEME

The one-dimensional steady-state convection-diffusion equation (without source or reaction terms) is

$$0 = \frac{d}{dx}\left(D(x)\frac{dV}{dx} \right) - v(x)\frac{dV}{dx} - V\frac{dv}{dx} \tag{1}$$

where $D(x)$ is the diffusion coefficient and $v(x)$ is the convection velocity, both of which are allowed to vary over space, x. The VI scheme is based on the similarity between this equation and the differential equation governing the voltage under steady-state conditions along a lossy transmission line (TL), i.e. a pair of conductors, with distributed resistance, capacitance and inductance $R_d(x)$, $C_d(x)$, and $L_d(x)$ respectively (all per unit length and varying with position, x), and with an additional distributed current source, $I_{Cd}(x)$ [5]

$$0 = \frac{d}{dx}\left(\frac{1}{R_d(x)C_d(x)}\frac{dV}{dx} \right) - \frac{d}{dx}\left(\frac{1}{C_d(x)} \right)\frac{1}{R_d(x)}\frac{dV}{dx} + \frac{I_{Cd}(x)}{C_d(x)} \tag{2}$$

This is equivalent to Equation (1) if the TL properties satisfy

$$D(x) = \left[R_d(x)C_d(x) \right]^{-1} \tag{3}$$

$$Pe(x) := \frac{v(x)}{D(x)} = C_d(x)\frac{d}{dx}\left(\frac{1}{C_d(x)} \right) \tag{4}$$

(where Pe is the Peclet number) and

$$V(x)\frac{dv}{dx} = -I_{Cd}(x)C_d(x)^{-1} \tag{5}$$

Modelling such a transmission line is equivalent to solving the convection-diffusion equation. It should be noted that the distributed inductance does not appear in Equation (2). The TLM method, however, used here to model the TL, requires a time step to be chosen, even if a steady-state solution is to be found directly, and this value determines the level of inductance [4, 5].

In the 1D TLM scheme, both space (i.e. the length of the TL) and time are divided into finite increments. Traditionally steady-state solutions have been found by running the scheme until transients reduce to an acceptable level [7, 10, 11], but a recent paper has shown that they can also be found directly [5]. The first step in modelling a transmission line using TLM is to choose the locations of the nodes at which the solution will be calculated and a time step length, Δt. The TL is then approximated by a network of discrete resistors, current sources, and uniform TL segments as illustrated in Figure 1. A pair of equal lossless TL segments (i.e. with zero resistance) connects each

pair of adjacent nodes. Two equal resistors located between these segments represent the distributed resistance of the TL being modelled. A discrete current source at each node represents the distributed current source.

A transmission line has both capacitance and inductance distributed along its length. The TLM scheme keeps track of individual voltage pulses that travel through the network. For simplicity the scheme is synchronised by arranging that all pulses leaving nodes at a given time step arrive at adjacent nodes Δt later. The propagation velocity is constant between adjacent nodes and therefore, at any point between two nodes Δx apart, must equal $\Delta x/\Delta t$. The propagation velocity, $u(x)$, of a TL is

$$u(x) = \left[L_d(x) C_d(x)\right]^{-\frac{1}{2}} \tag{6}$$

and so, once $C_d(x)$ has been found by solving Equation (4), this relationship can be used to determine the required distributed inductance.

In practice it is not necessary to know the distributed inductance and the distributed capacitance to model a TL using the TLM method. The important parameter that links the two is the distributed impedance

$$Z(x) = \left[L_d(x) C_d^{-1}(x)\right]^{\frac{1}{2}} \tag{7}$$

Combining Equations (6), (7), and $u(x) = \Delta x/\Delta t$, gives the impedance at a point x between two nodes Δx apart as

$$Z(x) = \Delta t/\left(\Delta x C_d(x)\right) \tag{8}$$

Once the values of the distributed resistance, impedance, and current source, are known, it is possible to determine the properties of the discrete components in the equivalent TLM network [4, 5]. The pair of resistors between each pair of nodes must have the same total resistance as the equivalent section of the TL being modelled. The impedance of the two TL segments must equal the average impedance of the TL between the two nodes. The current from the current source at node n must equal the sum of that from the distributed current source between nodes $n-1$ and n that flows to the right and that from the distributed current source between nodes n and $n+1$ that flows to the left [5].

Before these values can be calculated, an ODE that depends on $Pe(x)$ (Equation (4)) must be solved to find $C_d(x)$. To calculate the average impedance and the total resistance between nodes, it is necessary to integrate the result over space. If $Pe(x)$ varies over space then a closed-form solution of Equation (4) may not be available and the cost of calculating the parameter values numerically is similar to that of solving the CDE itself. Two efficient, but less accurate, alternatives have been developed. In the first it is assumed that v and D are both constant over space when deriving the necessary equations and in the second it is assumed that v and D vary in a piecewise-constant

fashion [5]. These have allowed straightforward relationships to be developed between the CDE coefficients, v and D, and the parameters required for the TLM model. The second method is generally the more accurate of the two but the cost of parameter calculation is higher.

To understand what parameters are required for a TLM model, it is first necessary to understand how the method is implemented. The scheme keeps track of Dirac voltage pulses that travel through the network. At any time step, k, there are voltage pulses incident at node n, one from the left (${}_kVil_n$) and one from the right (${}_kVir_n$). These instantaneously raise the "node voltage" (${}_kVn_n$), which is common to the lines meeting at the node, to [5]

$$ {}_kVn_n = \frac{2_kVil_n + 2P_{n\,k}Vir_n + Z_{n\,k}I_{Cn}}{1+P_n} \tag{9} $$

where ${}_kI_{Cn}$ is the current supplied from the current source at that time step and where $P_n = Z_n/Z_{n+1}$ is the "impedance ratio" at node n. The values of Vn, along the line and over time, represent the time-domain solution of the equation being modelled. The difference between the instantaneous node voltage and the incident voltages leads to pulses being scattered from the node, one to the left

$$ {}_kVsl_n = {}_kVn_n - {}_kVil_n \tag{10} $$

and one to the right

$$ {}_kVsr_n = {}_kVn_n - {}_kVir_n \tag{11} $$

Pulses pass unmodified along the TL segments. Any pulse leaving a node will arrive at an impedance discontinuity $\frac{1}{2}\Delta t$ later (i.e. when it has travelled the length of one TL segment) due to the presence of the resistors in the network. A fraction τ (the transmission coefficient, where $0 \leq \tau < 1$) travels on, arriving at the adjacent node at the next time step. The remaining fraction $(1-\tau)$ is reflected back, arriving at the node from which it originated at the next time step. The equations for the incident pulses at node n at time step $k+1$ (generally referred to as the "connection equations" for the network) are therefore

$$ {}_{k+1}Vil_n = (1-\tau_n)\,{}_kVsl_n + \tau_{n\,k}Vsr_{n-1}, \quad {}_{k+1}Vir_n = (1-\tau_{n+1})\,{}_kVsr_n + \tau_{n+1\,k}Vsl_{n+1} \tag{12} $$

where τ_n, the transmission coefficient for connecting line n (i.e. the line between nodes $n-1$ and n), is $\tau_n = Z_n/(Z_n + R_n)$.

Now ${}_kI_{Cn}$ is an integral of $I_{Cd}(x)$ between nodes $n-1$ and $n+1$ at time step k [5]. This distributed current is, from Equation (5), proportional to $V(x)$ at that time step. To simplify the method, it has been assumed in calculating ${}_kI_{Cn}$ that $V(x)$ between nodes $n-1$ and $n+1$ at time step k is equal to ${}_kVn_n$. This allows the introduction of a new node parameter, Y_n, such that

$$ Z_{n\,k}I_{Cn} = Y_{n\,k}Vn_n \tag{13} $$

and so Equation (9) can be rewritten as

$$ {}_kVn_n = \frac{2_kVil_n + 2P_n{}_kVir_n}{1 + P_n + Y_n} \tag{14} $$

A time-domain model is initiated by setting the two incident voltages at each node equal to half the desired initial node voltage distribution along the line. Equation (14) is used to calculate the resulting node voltages, then Equations (10) and (11) give the scattered voltages, and Equation (12) gives the incident voltages for the next time step. These are then used to calculate the new node voltages and so on. If a steady state is reached (which will depend on the boundary conditions) the incident pulses at time step k will equal those at time step $k-1$. This fact allows the determination of equations for the steady-state incident voltages at each node, ${}_\infty Vil_n$ and ${}_\infty Vir_n$ [5]

$$ a_{nl\infty}Vil_{n-1} + b_{nl\infty}Vir_{n-1} - {}_\infty Vil_n + c_{nl\infty}Vir_n = 0\,,\ 2 \le n \le N \tag{15} $$

$$ a_{nr\infty}Vil_n - {}_\infty Vir_n + b_{nr\infty}Vil_{n+1} + c_{nr\infty}Vir_{n+1} = 0\,,\ 1 \le n \le N-1 \tag{16} $$

where

$$ \begin{gathered} a_{nl} = \frac{2\sigma_{2,n}\tau_n}{\sigma_{7,n}}\,,\ b_{nl} = \frac{a_{nl}}{2}\sigma_{5,n-1}\,,\ c_{nl} = \frac{2\sigma_{9,n}(1-\tau_n)}{\sigma_{7,n}}\,, \\ a_{nr} = \frac{2\sigma_{2,n+1}(1-\tau_{n+1})}{\sigma_{8,n}}\,,\ b_{nr} = \frac{\sigma_{2,n}\sigma_{6,n+1}}{\sigma_{8,n}}\,,\ c_{nr} = \frac{2\sigma_{9,n+1}\tau_{n+1}}{\sigma_{8,n}} \end{gathered} \tag{17} $$

and

$$ \begin{gathered} \sigma_{1,n} = P_n + Y_n\,,\ \sigma_{2,n} = 1 + \sigma_{1,n}\,,\ \sigma_{3,n} = 1 + \sigma_{2,n}\,,\ \sigma_{4,n} = Y_n + 1\,,\ \sigma_{5,n} = P_n - \sigma_{4,n}\,,\ \sigma_{6,n} = \sigma_{3,n}\tau_n\,, \\ \sigma_{7,n} = \sigma_{2,n-1}(\sigma_{6,n} + 2\sigma_{1,n})\,,\ \sigma_{8,n} = \sigma_{2,n+1}(\sigma_{5,n}\tau_{n+1} + 2\sigma_{4,n})\,,\ \sigma_{9,n} = P_n\sigma_{2,n-1} \end{gathered} \tag{18} $$

It can be seen that, once the values of Y_n, τ_n, and P_n, are determined, it takes a further minimum of 8 additions/subtractions and 23 multiplications/divisions to calculate the coefficients in Equations (15) and (16) for each node.

To solve the resulting equations the boundary conditions must first be implemented. To impose Dirichlet boundary conditions, nodes can be located at each boundary and the node voltages at those nodes simply fixed at the required values. It is not necessary to locate nodes at the boundaries but this does simplify the scheme [4]. The implementation of other types of boundary conditions is not considered here.

The steady-state equations can be written in terms of ${}_\infty Vil_n$ and ${}_\infty Vir_n$ as shown above, and modified as necessary at the boundaries. They can also be written in terms of ${}_\infty Vil_n$ and ${}_\infty Vn_n$ or of ${}_\infty Vir_n$ and ${}_\infty Vn_n$. Testing suggests that there is very little benefit, if any, from doing so, in terms of the overall cost of the scheme.

Before modelling can begin, it is necessary to calculate P_n and Y_n for each node and τ_n for each connecting line. It has been shown previously that, if Pe and D are assumed to be constant, then [4]

$$\tau_n = \frac{1}{1+\frac{1}{2}D^{-1}\Delta x_n^2 \Delta t^{-1}} \tag{19}$$

If D varies over space then the average of D_n and D_{n+1}, the values at the nodes at the ends of the connecting line, can be used to calculate τ_n. The impedance ratio at node n is

$$P_n = \frac{\Delta x_{n+1}^2}{\Delta x_n^2}\frac{A_n}{B_n} \tag{20}$$

where

$$A_n = 1-\exp\left(-Pe\Delta x_n\right),\ \ B_n = \exp\left(Pe\Delta x_{n+1}\right)-1 \tag{21}$$

If Pe varies over space then its value at node n can be used when calculating P_n. If Pe is zero at any node n then $P_n = \Delta x_{n+1}/\Delta x_n$. Assuming dv/dx is also constant over space gives [5]

$$Y_n = \frac{dv}{dx}\left[1-\frac{\Delta x_{n+1}}{\Delta x_n}\frac{A_n}{B_n}\right]\frac{\Delta t}{Pe\Delta x_n} \tag{22}$$

or, if $Pe = 0$, $Y_n = \frac{1}{2}(dv/dx)\Delta t(\Delta x_{n+1} + \Delta x_n)/\Delta x_n$. The VI method as implemented using these equations is referred to here as the $\mathrm{VI_C}$ scheme.

Another possibility, the $\mathrm{VI_{PC}}$ scheme, assumes that both parameters (i.e. v and D) vary in a piecewise-constant fashion so that $Pe(x) = Pe_n$ and $D(x) = D_n$ between $x_n - \frac{1}{2}\Delta x_n$ and $x_n + \frac{1}{2}\Delta x_{n+1}$. With these assumptions [5]

$$P_n = \frac{Pe_{n+1}\Delta x_{n+1}^2 \alpha_{7,n}}{Pe_{n-1}\Delta x_n^2 \alpha_{8,n+1}} \tag{23}$$

where

$$\begin{gathered}\alpha_{1,n} = \exp\left(-\tfrac{1}{2}Pe_n\Delta x_n\right),\ \ \alpha_{2,n} = \exp\left(-\tfrac{1}{2}Pe_{n-1}\Delta x_n\right),\ \ \alpha_{3,n} = \left(\alpha_{1,n}-1\right)Pe_{n-1}\,, \\ \alpha_{4,n} = \left(\alpha_{2,n}-1\right)Pe_n\,,\ \ \alpha_{5,n} = \left(1-1/\alpha_{1,n}\right)Pe_{n-1}\,,\ \ \alpha_{6,n} = \left(1-1/\alpha_{2,n}\right)Pe_n\,, \\ \alpha_{7,n} = \alpha_{1,n}\alpha_{4,n} + \alpha_{3,n}\,,\ \ \alpha_{8,n} = \alpha_{6,n} + \alpha_{5,n}/\alpha_{2,n}\end{gathered} \tag{24}$$

and the equivalent transmission coefficient is [5]

$$\tau_n = \frac{2}{2+\frac{\Delta x_n^2}{\Delta t}\left(\frac{\alpha_{4,n}/D_{n-1} + \alpha_{5,n}/D_n}{\alpha_{4,n}+\alpha_{5,n}}\right)} \tag{25}$$

Note that the limits of $\alpha_{4,n}$ and $\alpha_{5,n}$, as Pe_n and Pe_{n-1}, respectively, go to zero, are both $\frac{1}{2}\Delta x_n$. If dv/dx also varies in a piecewise-constant fashion (consistent with that described above) then [5]

$$Y_n = \Delta t\left(\Gamma_{1,n}\frac{dv}{dx}_{n-1} + \Gamma_{2,n}\frac{dv}{dx}_{n} + \Gamma_{3,n}\frac{dv}{dx}_{n+1}\right) \tag{26}$$

where

$$\Gamma_{1,n} = \frac{\alpha_{2,n} + \frac{1}{2}Pe_{n-1}\Delta x_n - 1}{\left(Pe_{n-1}\Delta x_n\right)^2},\ \Gamma_{3,n} = -\alpha_{7,n}\frac{\alpha_{5,n+1}/Pe_n + \frac{1}{2}Pe_{n+1}\Delta x_{n+1}}{Pe_{n-1}Pe_{n+1}\Delta x_n^2\alpha_{8,n+1}},$$
$$\Gamma_{2,n} = \frac{\alpha_{7,n} - \alpha_{4,n} + \frac{1}{2}\alpha_{9,n}}{\alpha_{9,n}Pe_n\Delta x_n} + \alpha_{7,n}\frac{\alpha_{5,n+1} - \alpha_{8,n+1} - \frac{1}{2}\alpha_{9,n+1}}{\alpha_{9,n}Pe_n\Delta x_n\alpha_{8,n+1}} \tag{27}$$

and $\alpha_{9,n} = Pe_{n-1}Pe_n\Delta x_n$. If $Pe_n = 0$ for all nodes then this simplifies to

$$\lim_{Pe\to 0} Y_n = \tfrac{1}{8}\Delta t\left[\Delta x_n\left(\frac{dv}{dx}_{n-1} + 3\frac{dv}{dx}_n\right) + \Delta x_{n+1}\left(\frac{dv}{dx}_{n+1} + 3\frac{dv}{dx}_n\right)\right]\Delta x_n^{-1} \tag{28}$$

It is clear that the VI_C scheme has a significantly lower computational cost than the VI_{PC} scheme.

THE CONVECTION LINE METHOD

The novel method introduced here combines a standard lossy TLM diffusion model, composed of a series of TL segments and resistors, with a second lossless (i.e. with zero resistance) transmission line which essentially models convection. The two lines, referred to here as the "diffusion line" and the "convection line" are connected at each node as shown in Figure 2. Each section of the convection line has a notional diode, used previously in TLM to model waves in moving media [12, 13], which allows pulses (either positive or negative) to travel in one direction only.

The diffusion line is essentially a standard lossy TLM network for modelling diffusion and is equivalent to a VI network with $v = 0$. All TL segment impedances are therefore equal unless the nodes are unequally spaced. The impedance ratio, defined as for the VI scheme, at node n is $P_n = \Delta x_{n+1}/\Delta x_n$.

There are three incident voltage pulses at node n at time step k, ${}_kVil_n$ and ${}_kVir_n$ arriving from the diffusion line, and ${}_kVilc_n$ arriving from the section of convection line to the left of the node. There are also three scattered pulses, ${}_kVsl_n$, ${}_kVsr_n$, and ${}_kVsrc_n$ which is scattered to the right along the convection line. The presence of the diodes, and the absence of resistors, ensure that there are no pulses, either incident or scattered, travelling to the left along the convection line.

The voltage pulses in such a network must obey two physical laws. Firstly, the total current associated with the incident pulses (i.e. the voltage divided by the impedance) must equal the total current associated with the scattered pulses, and so

$$\frac{{}_kVil_n}{Z_n} + \frac{{}_kVir_n}{Z_{n+1}} + \frac{{}_kVilc_n}{Z_{c,n}} = \frac{{}_kVsl_n}{Z_n} + \frac{{}_kVsr_n}{Z_{n+1}} + \frac{{}_kVsrc_n}{Z_{c,n+1}} \tag{29}$$

which can be rewritten as

$$\frac{{}_kVil_n}{Z_n} + \frac{{}_kVir_nP_n}{Z_n} + \frac{{}_kVilc_nQ_n}{Z_n} = \frac{{}_kVsl_n}{Z_n} + \frac{{}_kVsr_nP_n}{Z_n} + \frac{{}_kVsrc_nP_nQ_{n+1}}{Z_n} \tag{30}$$

where Q_n is called here the "convection/diffusion impedance ratio" for "connecting line" n (i.e. the line between nodes $n-1$ and n) and equals $Z_n / Z_{c,n}$. Secondly, a node voltage must equal the sum of the incident and scattered voltage pulses on each TL segment connected to the node. This gives the scattering equations for the network

$$ {}_kVsl_n = {}_kVn_n - {}_kVil_n, \quad {}_kVsr_n = {}_kVn_n - {}_kVir_n, \quad {}_kVsrc_n = {}_kVn_n \tag{31} $$

Note that this rule does not apply to TL segments connected to a node through a diode (i.e. ${}_kVn_n$ need not equal ${}_kVilc_n$). Combining Equations (30) and (31) gives

$$ {}_kVn_n = \frac{2\,{}_kVil_n + 2P_n\,{}_kVir_n + Q_n\,{}_kVilc_n}{1 + P_n + P_nQ_{n+1}} \tag{32} $$

The connection equations for the diffusion line pulses are the same as for the VI scheme (i.e. Equation (12)), while that for the convection line is simply

$$ {}_{k+1}Vilc_n = {}_kVsrc_{n-1} = {}_kVn_{n-1} \tag{33} $$

Under steady-state conditions, the diffusion line incident pulses and the node voltages stay the same from one time-step to the next. It can be easily shown that the steady-state values of *Vir*, *Vn*, and *Vil* for node *n* must therefore satisfy

$$ \tau_n\,{}_\infty Vn_{n-1} - \tau_n\,{}_\infty Vir_{n-1} + (\tau_n - 2)\,{}_\infty Vil_n + (1-\tau_n)\,{}_\infty Vn_n = 0 \tag{34} $$

$$ -Q_n\,{}_\infty Vn_{n-1} - 2\,{}_\infty Vil_n + (1 + P_n + P_nQ_{n+1})\,{}_\infty Vn_n - 2P_n\,{}_\infty Vir_n = 0 \tag{35} $$

$$ (1-\tau_{n+1})\,{}_\infty Vn_n + (\tau_{n+1} - 2)\,{}_\infty Vir_n - \tau_{n+1}\,{}_\infty Vil_{n+1} + \tau_{n+1}\,{}_\infty Vn_{n+1} = 0 \tag{36} $$

If these equations are instead written in terms of ${}_\infty Vir_n$, ${}_\infty Vil_n$, and ${}_\infty Vilc_n$, the result is significantly more complex (the fact that ${}_\infty Vilc_n$ equals ${}_\infty Vn_{n-1}$ allows for their simplification). When written for all N nodes in a model, and suitably modified for the boundary nodes (discussed below), these equations can be solved to get the steady-state node voltages directly.

Once the P_n, Q_n, and τ_n values are calculated, there are only 4 additions/subtractions and 2 multiplications/divisions required to calculate the coefficients for each internal node (significantly lower than for the VI scheme). The cost of solving the equations is, however, greater than for the VI method since there are now 3 equations per node instead of 2.

The implementation of Dirichlet boundaries is straightforward if nodes are located at the boundaries, the boundary node voltages being simply fixed at the required value and the steady-state equations altered accordingly.

Convection velocity

In order to determine the relationships between the values of P_n, Q_n, and τ_n, and the values of $D(x)$ and $v(x)$, it is useful to first examine the case where there is zero diffusion. Consider an infinite

model with uniformly spaced nodes (i.e. P_n = 1 throughout), with Q the same for all connecting lines, and with τ = 0 for all diffusion line sections. Voltage pulses can only move from one node to the next along the convection-line in such a network, but voltage pulses are also scattered into the diffusion line TL segments at each time step, arriving back at the next time step. It is clear that the shape of the node voltage profile will be affected over time by this process. The effective convection velocity can be determined by measuring the change in the mean position of the node voltage profile in a single time step.

Let ${}_k\varsigma_{Vil} = \sum {}_k Vil_n$, the sum of the voltage pulses incident from the left at all nodes in the model at time step *k*. Similarly let ${}_k\varsigma_{Vir} = \sum {}_k Vir_n$ and ${}_k\varsigma_{Vilc} = \sum {}_k Vilc_n$. The sum of the node voltages at time step *k* is then

$$ {}_k\varsigma_{Vn} = \frac{2_k\varsigma_{Vil} + 2_k\varsigma_{Vir} + Q_k\varsigma_{Vilc}}{2+Q} \tag{37} $$

The sums of the scattered pulses are ${}_k\varsigma_{Vsr} = {}_k\varsigma_{Vn} - {}_k\varsigma_{Vir}$, ${}_k\varsigma_{Vsl} = {}_k\varsigma_{Vn} - {}_k\varsigma_{Vil}$, and ${}_k\varsigma_{Vsrc} = {}_k\varsigma_{Vn}$. The sums of the incident pulses at the next time step are ${}_{k+1}\varsigma_{Vil} = {}_k\varsigma_{Vsl}$, ${}_{k+1}\varsigma_{Vir} = {}_k\varsigma_{Vsr}$, and ${}_{k+1}\varsigma_{Vilc} = {}_k\varsigma_{Vn}$. Combining these equations to get ${}_{k+1}\varsigma_{Vn}$ in terms of the sums of the incident pulses at time step *k* gives

$$ {}_{k+1}\varsigma_{Vn} = \frac{4_k\varsigma_{Vil} + 4_k\varsigma_{Vir} + \left(4Q+Q^2\right)_k\varsigma_{Vilc}}{\left(2+Q\right)^2} \tag{38} $$

For the method to be conservative, ${}_{k+1}\varsigma_{Vn}$ must equal ${}_k\varsigma_{Vn}$ (i.e. the sum of the node voltages in an infinitely long model must remain constant over time). From Equations (37) and (38), this condition is equivalent to ${}_k\varsigma_{Vil} + {}_k\varsigma_{Vir} = {}_k\varsigma_{Vilc}$. If the model is not initialised with incident voltage pulses that satisfy this condition then the sum of the node voltages will change from one time step to the next. If this condition is satisfied then the equations above give ${}_{k+1}\varsigma_{Vil} = {}_k\varsigma_{Vir}$, ${}_{k+1}\varsigma_{Vir} = {}_k\varsigma_{Vil}$, and ${}_{k+1}\varsigma_{Vilc} = {}_k\varsigma_{Vilc}$. If ${}_k\varsigma_{Vil} = {}_k\varsigma_{Vir} = \frac{1}{2}{}_k\varsigma_{Vilc}$ then all three sums will remain constant from one time step to the next. Only this case is examined here.

If ${}_k\bar{n}_{Vil}$ is the mean position of the *Vil* voltage pulse profile at time step *k* (in terms of node number, where the nodes are numbered sequentially from left to right), and ${}_k\bar{n}_{Vir}$ and ${}_k\bar{n}_{Vilc}$ are the mean positions of the other incident voltage pulse profiles, then the mean position of the node voltage profile is

$$ {}_k\bar{n}_{Vn} = \frac{2_k\varsigma_{Vil}\,{}_k\bar{n}_{Vil} + 2_k\varsigma_{Vir}\,{}_k\bar{n}_{Vir} + Q_k\varsigma_{Vilc}\,{}_k\bar{n}_{Vilc}}{2_k\varsigma_{Vil} + 2_k\varsigma_{Vir} + Q_k\varsigma_{Vilc}} = \frac{{}_k\bar{n}_{Vil} + {}_k\bar{n}_{Vir} + Q_k\bar{n}_{Vilc}}{2+Q} \tag{39} $$

The mean positions of the incident voltage pulse profiles at the next time step can easily be determined from the equations for scattering and connection given above

$$\begin{aligned} {}_{k+1}\overline{n}_{Vir} = {}_{k}\overline{n}_{Vsr} &= \left({}_{k}\varsigma_{Vn\,k}\,{}_{k}\overline{n}_{Vn} - {}_{k}\varsigma_{Vir\,k}\,{}_{k}\overline{n}_{Vir}\right)/\left({}_{k}\varsigma_{Vn\,k} - {}_{k}\varsigma_{Vir\,k}\right), \\ {}_{k+1}\overline{n}_{Vil} = {}_{k}\overline{n}_{Vsl} &= \left({}_{k}\varsigma_{Vn\,k}\,{}_{k}\overline{n}_{Vn} - {}_{k}\varsigma_{Vil\,k}\,{}_{k}\overline{n}_{Vil}\right)/\left({}_{k}\varsigma_{Vn\,k} - {}_{k}\varsigma_{Vil\,k}\right), \\ {}_{k+1}\overline{n}_{Vilc} = {}_{k}\overline{n}_{Vsrc} + 1 &= {}_{k}\overline{n}_{Vn} + 1 \end{aligned} \tag{40}$$

These can be used to find the mean position of the node voltage profile at time step k+1

$${}_{k+1}\overline{n}_{Vn} = \frac{2\,{}_{k}\overline{n}_{Vil} + 2\,{}_{k}\overline{n}_{Vir} + Q(Q+4)\,{}_{k}\overline{n}_{Vilc} + Q(2+Q)}{(2+Q)^2} \tag{41}$$

If ${}_{k}v'$ is the change in mean position during time step k (i.e. if ${}_{k}v' = {}_{k+1}\overline{n}_{Vn} - {}_{k}\overline{n}_{Vn}$), then Equations (39) and (41) give

$${}_{k}v' = \frac{Q\left({}_{k}\Delta\overline{n} + 2 + Q\right)}{(2+Q)^2} \tag{42}$$

where ${}_{k}\Delta\overline{n} = 2\,{}_{k}\overline{n}_{Vilb} - {}_{k}\overline{n}_{Vil} - {}_{k}\overline{n}_{Vir}$. Equation (40) can be used to find ${}_{k+1}\Delta\overline{n}$ in terms of ${}_{k}\Delta\overline{n}$

$${}_{k+1}\Delta\overline{n} = \frac{4 + 2Q - Q\,{}_{k}\Delta\overline{n}}{2+Q} \tag{43}$$

Testing has shown that ${}_{k}v'$, measured for such a model, varies initially from one time step to the next before converging to a constant value, denoted ${}_{\infty}v'$. Similar behaviour has been demonstrated previously in the effective diffusion rate in standard lossy TLM models [14]. From Equation (42), ${}_{k}v'$ cannot be constant over time unless ${}_{k}\Delta\overline{n}$ is also constant. From Equation (43), ${}_{k}\Delta\overline{n}$ can be constant only if it equals (2+Q)/(1+Q). Substituting this for ${}_{k}\Delta\overline{n}$ in Equation (42) gives ${}_{\infty}v' = Q/(1+Q)$. This is the change in the node profile mean position, in terms of node number, from one time step to the next for k >> 1. The modelled convection velocity, once ${}_{k}v'$ has converged to this value, is therefore simply

$$v = \frac{Q}{1+Q}\frac{\Delta x}{\Delta t} \tag{44}$$

Testing has shown that this equation also holds when ${}_{k}\varsigma_{Vil} \neq {}_{k}\varsigma_{Vir}$, and, more generally, when $\tau_n \neq 0$ (i.e. when diffusion is being modelled as well as convection). The latter is not surprising since diffusion is symmetrical. While it affects the mean positions of the *Vil* and *Vir* profiles [14], it does not affect their sum (and so does not affect ${}_{k}\Delta\overline{n}$).

Equation (44) allows the value of Q to be chosen for a model for any desired convection velocity

$$Q_n = \frac{v_n \Delta t / \Delta x_n}{1 - v_n \Delta t / \Delta x_n} \tag{45}$$

where v_n is the value of the velocity used to calculate the ratio Q for connecting line n.

It should be noted that an equation for the convection velocity in the VI scheme, derived in a similar manner (i.e. from the change in mean position of the solution profile over time under purely transient conditions), does not match the convection velocity exhibited by that scheme under steady-state conditions [15]. Test results presented below suggest that in the CL scheme there is no such difference between the rates of convection under transient and steady-state conditions.

Convection-related errors

Further useful information can be gleaned from the steady-state solution of such a model. For the case where $\tau = 0$ for all connecting lines, Equations (34) to (36) simplify to

$${}_{\infty}Vn_n = \frac{Q_n}{P_n Q_{n+1}} {}_{\infty}Vn_{n-1} \tag{46}$$

Now the solution of Equation (1) with $D = 0$ is $V(x)=c/v(x)$, where c is a constant, and so the exact solution at nodes n and $n-1$ will satisfy

$${}_{\infty}Vn_n = \frac{v(x_{n-1})}{v(x_n)} {}_{\infty}Vn_{n-1} \tag{47}$$

Using Equation (45) for Q_n and Q_{n+1} allows Equation (46) to be rewritten as

$${}_{\infty}Vn_n = \frac{v_{n+1}\Delta t - P_n \Delta x_n}{v_{n+1} P_n \Delta t - v_{n+1} \Delta x_n / v_n} {}_{\infty}Vn_{n-1} \tag{48}$$

It is clear from comparing this with Equation (47) that an exact solution of the convection equation will only be obtained if $\Delta t = 0$ and if $v_{n+1} = v(x_n)$ and $v_n = v(x_{n-1})$ (i.e. if the convection velocity used to calculate Q for the convection line between nodes n and $n+1$, is that at node n).

Defining $\Delta Vn_{n/n-1}$ as the error in the ratio ${}_{\infty}Vn_n / {}_{\infty}Vn_{n-1}$ (i.e. as the difference between the actual ratio as given by Equation (48) and the desired ratio as given by Equation (47)) gives, for the case where $v_n = v(x_{n-1})$ and all nodes are evenly spaced,

$$\Delta Vn_{n/n-1} = \frac{v_{n+1}\Delta t - \Delta x}{v_{n+1}\Delta t - v_{n+1}\Delta x / v_n} - \frac{v_n}{v_{n+1}} = \frac{v_n \Delta t (v_{n+1} - v_n)}{v_{n+1}(v_n \Delta t - \Delta x)} \tag{49}$$

The error in the value of the solution at node n will depend on this and on the error in Vn_{n-1}. It will be infinite if $v_n \Delta t = \Delta x$. If $v_n \Delta t >> \Delta x$ then $\Delta Vn_{n/n-1} \approx (v_{n+1} - v_n)/v_{n+1}$, a function of the spatial variation in $v(x)$ and the node spacing. If $v_n \Delta t << \Delta x$ then $\Delta Vn_{n/n-1} \approx v_n \Delta t (v_n - v_{n+1})/(v_{n+1}\Delta x)$, i.e. the error decreases linearly with Δt.

Although setting $v_{n+1} = v(x_n)$ gives accurate results when $D = 0$ and Δt is very small (in practice the time step cannot be zero), testing has shown that setting $v_{n+1} = \frac{1}{2}[v(x_n)+ v(x_{n+1})]$ gives significantly more accurate results when $D \neq 0$. Under such circumstances, again assuming evenly spaced nodes, the ratio error is

$$\Delta Vn_{n/n-1} = \frac{\frac{1}{2}\left[v(x_n)+v(x_{n+1})\right]\Delta t - \Delta x}{\frac{1}{2}\left[v(x_n)+v(x_{n+1})\right]\Delta t - \left[v(x_n)+v(x_{n+1})\right]\Delta x/\left[v(x_{n-1})+v(x_n)\right]} - \frac{v(x_{n-1})}{v(x_n)} \tag{50}$$

If $\frac{1}{2}\left[v(x_n)+v(x_{n+1})\right]\Delta t << \Delta x$ then this is approximately

$$\lim_{\Delta t\to 0} \Delta Vn_{n/n-1} = \frac{\left[v(x_{n-1})+v(x_n)\right]}{\left[v(x_n)+v(x_{n+1})\right]} - \frac{v(x_{n-1})}{v(x_n)} \tag{51}$$

If $\frac{1}{2}\left[v(x_n)+v(x_{n+1})\right]\Delta t >> \Delta x$ then $\Delta Vn_{n/n-1} \approx \left[v(x_{n+1})-v(x_n)\right]/v(x_{n+1})$. The error goes to infinity if $\Delta t = 2\Delta x/\left[v(x_n)+v(x_{n+1})\right]$ for any node. Note that this corresponds to Q_n being infinite. The ratio error is zero for a certain value of Δt, but this is dependent on the local velocity values and will, in general, vary from one node to the next. There will, therefore, be no time step length that produces an exact result at all nodes, but there may be an optimum time step. There is no efficient way, however, to determine its value for a given problem.

The errors in the solution will be a function of the ratio errors at each node. Figure 3a shows the maximum error in results from models over the domain $x \in [0,1]$ with initial condition $Vn_1 = 1$, with $v(x) = 5+5x$, and with $N = 11$, while Figure 3b shows results from the same model with $N = 81$. It can be seen that the optimum time step decreases as Δx is decreased.

The ratio error at lower Δt values for the case where $v(x) = a + bx$ is (from Equation (51))

$$\lim_{\Delta t\to 0} \Delta Vn_{n/n-1} = \frac{\left[2v(x_n)-b\Delta x\right]}{\left[2v(x_n)+b\Delta x\right]} - \frac{v(x_n)-b\Delta x}{v(x_n)} = \frac{b^2\Delta x^2}{v(x_n)\left[2v(x_n)+b\Delta x\right]} \tag{52}$$

The local error at each step is, therefore, on the order of Δx^2 (assuming $b\Delta x << 2v(x_n)$). The global error at any point in space (for a low value of Δt) will consequently be on the order of Δx. Test results (including those in Figure 3) have confirmed that this is the case.

While these findings are for the specific case $D = 0$, it will be shown below that they are useful for understanding the errors that occur in the solution of the convection-diffusion equation when $v(x)$ varies over space. Importantly, they suggest that, unlike the VI method, this scheme inherently models the two convection-related terms in Equation (1) without the need for current sources.

Diffusion coefficient

It is necessary to determine the relationship between the rate of diffusion modelled under steady-state conditions and the transmission coefficient, τ, as a model parameter. It is clear that connecting the convection line to the diffusion line in a CL model affects the behaviour of the diffusion line, and

so the relationship between τ and D will not be the same as for a diffusion line with no convection line attached (as given in Equation (19)) .

It has been found that, as with the VI scheme, the CL method produces an exact solution to the steady-state convection-diffusion equation when both v and D are constant over space (see [4] and results presented below). This has allowed the relationship between D and τ to be determined empirically. The analytical solution of the steady-state convection-diffusion equation with both v and D constant and with boundary conditions, $V(0) = 0$ and $V(\lambda) = 1$, is

$$V(x) = \frac{\exp(xPe) - 1}{\exp(\lambda Pe) - 1} \tag{53}$$

A TLM model with constant v and D, and with evenly spaced nodes (Δx apart), will have the same transmission coefficient, τ, for all sections of the diffusion line, and will have the same value of Q for all sections of the convection line. By calculating solutions from models with $V(0) = 0$ and $V(\lambda) = 1$ and with different values of τ and Q, and comparing them with Equation (53), the following relationship has been found

$$\tau = \frac{2Q}{\exp(Pe\Delta x) - 1 + 2Q} \tag{54}$$

Note that with $v = 0$, this becomes equal to Equation (19). Time-domain results suggest that, with $v \neq 0$, the effective rate of diffusion under transient conditions differs from this. Such a difference also occurs with the VI method [15]. A study of these differences and a discussion of possible reasons for them are beyond the scope of this paper.

EXAMPLE

To illustrate the steps required in implementing the CL method an example is included here. Consider the case where $D(x) = 1$, $v(x) = 5 + 5x$, $V(0) = V_L$, $V(1) = V_R$, $N = 4$, and the nodes are evenly spaced (giving $\Delta x = 1/3$ and $P_n = 1$ for all nodes). The first step is to calculate the value of Q for each of the three connecting lines using Equation (45). A time step is required and the value $\Delta t = 1\times10^{-9}$ has been used in this example (the choice of time step for the method is considered in the next section). For all tests reported here, the value v_n used when calculating Q_n is the average of the convection velocities at nodes $n-1$ and n. This method of parameter calculation is consistent with that used for the VI_C scheme. With these settings Equation (45) gives, approximately, $Q_2 = 1.75000003\times10^{-8}$, $Q_3 = 2.25000005\times10^{-8}$, and $Q_4 = 2.75000008\times10^{-8}$. Equation (54) can now be used to calculate the corresponding transmission coefficients, with $Pe = v_n/D$ being used when calculating τ_n. This gives, approximately, $\tau_2 = 5.84331809\times10^{-9}$, $\tau_3 = 4.02414712\times10^{-9}$, and $\tau_4 = 2.71833441\times10^{-9}$. Writing Equations (34) to (36) for all internal nodes, and adding Equation (36) for ${}_\infty Vir_1$ and Equation (34) for ${}_\infty Vil_N$, gives the following system of eight equations

$$\begin{bmatrix} \tau_2-2 & -\tau_2 & \tau_2 & 0 & 0 & 0 & 0 & 0 \\ -\tau_2 & \tau_2-2 & 1-\tau_2 & 0 & 0 & 0 & 0 & 0 \\ 0 & -2 & 2+Q_3 & -2 & 0 & 0 & 0 & 0 \\ 0 & 0 & 1-\tau_3 & \tau_3-2 & -\tau_3 & \tau_3 & 0 & 0 \\ 0 & 0 & \tau_3 & -\tau_3 & \tau_3-2 & 1-\tau_3 & 0 & 0 \\ 0 & 0 & -Q_3 & 0 & -2 & 2+Q_4 & -2 & 0 \\ 0 & 0 & 0 & 0 & 0 & 1-\tau_4 & \tau_4-2 & -\tau_4 \\ 0 & 0 & 0 & 0 & 0 & \tau_4 & -\tau_4 & \tau_4-2 \end{bmatrix} \begin{bmatrix} {}_{\infty}Vir_1 \\ {}_{\infty}Vil_2 \\ {}_{\infty}Vn_2 \\ {}_{\infty}Vir_2 \\ {}_{\infty}Vil_3 \\ {}_{\infty}Vn_3 \\ {}_{\infty}Vir_3 \\ {}_{\infty}Vil_4 \end{bmatrix} = \begin{bmatrix} (\tau_2-1)V_L \\ -\tau_2 V_L \\ Q_2 V_L \\ 0 \\ 0 \\ 0 \\ -\tau_4 V_R \\ (\tau_4-1)V_R \end{bmatrix} \quad (55)$$

which, when solved with the coefficients for this example and with V_L = 0 and V_R = 1, give the results shown in Table 1. The exact solution is included along with equivalent results obtained using the VI_C and VI_{PC} schemes (both calculated using Δt = 1) and those from two standard second order finite difference (FD) schemes (one using centred-differences (CD) and one upwind-difference scheme (UP)).

This example (along with further tests reported below) suggests that the CL method is significantly more accurate than the VI schemes (which, in turn, as shown in Table 1, in further results below, and in results published previously [5], are significantly more accurate than FD methods when the convection term dominates). It is also clear from this example that the computational cost of the scheme is not excessive.

TESTING

From Equation (45), negative convection velocities require negative Q_n values (equivalent to having TL segments with negative impedance in the convection line). Testing has shown that, not surprisingly, a time-domain TLM model with negative Q_n values is unstable but despite this a steady-state solution can be found directly. Alternatively, negative convection velocities can be modelled while maintaining stability simply by changing the direction and position of the diodes in the TLM model. The former option has been used in the models tested here. Solutions in all cases have been found directly by solving the steady-state equations.

The test results below are for convection-diffusion equation problems which have analytical solutions available from symbolic maths software. The maximum errors quoted are $\max_{1\le n\le N}|V_n - Vn_n|$ where V_n represents the exact analytical solution at the location of node n.

Figure 4a shows the maximum errors in the solutions of models with v and D constant over space. It is clear that the errors in all three schemes tested are dependent on the choice of Δt. The close correspondence between the maximum error and the condition number, κ, for the systems of steady-state equations (Figure 4b), suggests that the solution errors are due to round-off errors in the calculation of the solution, the TLM parameters, and/or the steady-state equation coefficients. It

should be noted that the peak in the value of κ (and the corresponding peak in the maximum error) for the CL method corresponds to the point where $v\Delta t = \Delta x$ (and $Q_n = \infty$).

Figure 5a shows equivalent results from models with $D = 1$, $v = 5+5x$, and with 11 evenly spaced nodes. The analytical solution of Equation (1) with $v(x) = a + bx$, $V(0) = 0$ and $V(1) = 1$, is

$$V(x) = \exp\left[\frac{\frac{1}{2}(x-1)(2a+b(x+1))}{D}\right]\left[\frac{\operatorname{erf}\left(\frac{a}{\sqrt{2bD}}\right) - \operatorname{erf}\left(\frac{(a+bx)}{\sqrt{2bD}}\right)}{\operatorname{erf}\left(\frac{a}{\sqrt{2bD}}\right) - \operatorname{erf}\left(\frac{(a+b)}{\sqrt{2bD}}\right)}\right] \tag{56}$$

As expected [5] the VI_{PC} scheme is more accurate than the VI_C scheme. The round-off errors for the VI schemes are insignificant when compared with the systematic errors resulting from the spatial variation in $v(x)$ (except for very short time steps). This is not the case for the CL method. The systematic errors for the CL scheme are qualitatively similar to those for the case where $D = 0$ (Figure 3), i.e. there is a point at which the error is a minimum, points at which it is infinite (corresponding to $v_n\Delta t$ equalling Δx for one or more sections of the model), and the systematic error is relatively independent of Δt for both longer and shorter time steps. The round-off error is larger than the systematic errors for very small Δt values. The time step length for which the maximum error is a minimum is less than in the equivalent case with $D = 0$ (and decreases further as D is increased).

Figure 5 also illustrates a difficulty in determining the relationship between the systematic errors and the node spacing. Figure 5b shows results equivalent to those in Figure 5a but obtained from a model with 41 nodes instead of 11. In that case the values of Δt at which the error is low and independent of Δt correspond to values for which the round-off error is significant, and so the systematic error as Δt approaches zero cannot be determined empirically. It has been found, however, that the systematic errors in models with $D = 1$ and $v = 1/(1+x)$ can be measured (with a setting of $\Delta t = 10^{-9}$) over a relatively wide range of node spacings, thus allowing benchmarking of the scheme. The analytical solution with $V(0) = 0$ and $V(1) = 1$ is

$$V(x) = \frac{(1+x)\ln(1+x)}{2\ln(2)} \tag{57}$$

Table 2 contains results obtained from the three schemes with these settings (but with Δt set to 1 for the two VI schemes to avoid significant round-off errors) and with different numbers of evenly spaced nodes. These suggest that the errors associated with spatial variations in $v(x)$ are of the order of Δx^2 for all three schemes. The results of testing with $v(x) = a + bx$, although limited by round-off errors, also suggest that the CL scheme is at least second-order accurate. The analysis of the scheme with $D = 0$ presented above has shown that, under such circumstances, the method is first-order accurate. The reasons for this difference have not been investigated.

These results suggest that the equation giving the required value of Q for given values of v, as derived above for transient conditions with $D = 0$, is more generally applicable. They also confirm that this method can model both convection terms in the CDE.

Table 3 contains results obtained from models with constant $v(x)$ but with $D(x) = 1+x$. The analytical solution for this case, with $V(0) = 0$ and $V(1) = 1$, is

$$V(x) = \frac{(x+1)^v - 1}{2^v - 1} \tag{58}$$

Because there is no spatial variation in the velocity, the systematic errors in the results are independent of Δt and so a setting of $\Delta t = 1$ has been used for all three schemes. The CL method is, in most cases, significantly more accurate than either of the VI schemes. It is almost exactly twice as accurate as the VI_{PC} scheme for all v values for which results are presented (but testing has shown that this is not the case when $D(x)$ is changed to, for example, $1+x^2$). These results suggest that the ability of the TLM network to model the diffusion term in Equation (1) is not affected by the addition of the convection line. Results not given here suggest that the error resulting from a variation in $D(x)$ is second order for all three schemes.

All results from CL models presented below have been calculated using a time step of $\Delta t = 10^{-9}$ and all VI results have been calculated using a time step of $\Delta t = 1$. These have been chosen so that systematic errors are presented and not round-off errors (which are dependent on the specific way in which the calculations are performed).

It is clear from Table 3 that the accuracy of the TLM methods can decrease as the convection velocity increases. This is consistent with many traditional methods [1, 2, 3]. It has been shown previously, however, that this is not generally the case with the VI schemes [5]. Table 4 shows the errors in the solutions at 4 internal nodes obtained using the three TLM schemes and two FD schemes for three cases with $D(x)$ constant. It shows that with low Peclet numbers the accuracy of the VI_C and CD schemes are similar. Unlike the FD schemes, however, the accuracy of all three TLM methods increases as the convection velocity increases.

The CL models tested have convection lines with diodes directed to allow convection to the right. To model negative convection without changing diode directions, negative TL impedances are required. To check whether this affects the accuracy of the scheme under such circumstances, the results from a model with $V(0) = 1$, $V(1) = 0$, $D = 1$, and $v(x) = -5+5x$ have been compared with those from a model with $V(0) = 0$, $V(1) = 1$, $D = 1$, and $v(x) = 5x$. The two solutions are simply mirror images of each other, but in the first case the velocities are negative over the domain. Tests have shown that the maximum errors are identical. This suggests that, although the presence of negative TL impedances may affect the stability of a time-domain solution, it does not affect the accuracy of a directly obtained steady-state solution.

The equations given above for implementing all three schemes allow the node spacing, Δx, to vary along the model. By more closely spacing nodes where the solution (or the velocity and/or diffusion coefficient) has a higher gradient, it may be possible to achieve a required level of accuracy with fewer nodes. To test the effect of variations in node spacing, models with $\Delta x_n = m\Delta x_{n-1}$ (i.e. with Δx_n varying exponentially along the model), $v(x) = 5+5x$, $D = 1$, $N = 11$, $V(0) = 0$, and $V(1) = 1$, have been tested. With $m < 1$, these have nodes more closely spaced near the right-hand boundary where the solution varies most rapidly. Table 5 contains the maximum errors in the three schemes for these conditions for different values of m. Note that the first column gives the errors obtained with evenly spaced nodes. The accuracy of both the VI_{PC} and CL solutions decreases the more variation there is in Δx. This suggests that any advantage gained due to having more finely spaced nodes near the right-hand boundary is more than offset by errors occurring due to the spatial variation in Δx. The VI_C scheme, however, gives more accurate results as m is increased up to a point for this case. It is clear that the CL scheme is significantly more accurate than the VI schemes in all cases. It should be noted that (unlike with the VI schemes and with many traditional methods) the additional cost associated with variations in Δx in a CL model is insignificant.

All test results presented above are for CDEs for which analytical solutions are readily available. A more general test has been performed with $v(x) = 0.1 + x^4$, $D(x) = 1 + \sin(\pi x)$, $V(0) = 0$, and $V(1) = 1$. The solution at $x = 0.5$, calculated for a range of N values, has been compared with the solution at that point obtained using the VI_{PC} scheme with $N = 20001$. The magnitudes of the differences are given in Table 6. Results are given for the VI schemes in which the values of dv/dx at each node have been calculated analytically. It can be seen that the accuracy of the CL scheme is slightly less than that of the VI_{PC} scheme but is higher than that of the VI_C method. Since exact values of dv/dx will not generally be available, results are also given for the VI schemes with dv/dx calculated at each node using the values of $v(x)$ at the adjacent nodes and a standard second-order central-difference formula. It is clear that, under these circumstances, the CL method has performed significantly better then the VI schemes (which are then first-order accurate).

In all cases presented above, the maximum systematic error in the CL model solutions is lower as Δt approaches 0 than as Δt approaches infinity. Analysis of the case where $D = 0$ shows that this is not necessarily the case. Extensive testing has not, however, yielded settings for which this is not the case when $D \neq 0$. Why this might be so has not been investigated.

When $D = 0$ and v_n is set to $v(x_{n-1})$ for each connecting line, it has been shown above that the error in the CL scheme goes to zero as Δt goes to zero. Testing has shown that this is not the case when $D \neq 0$. In that case, if $v_n = v(x_{n-1})$, then the errors vary with Δt in a similar fashion to when $v_n = \frac{1}{2}[v(x_{n-1}) + v(x_n)]$, but are, in general, significantly larger.

DISCUSSION AND CONCLUDING REMARKS

The VI scheme is based on the similarity, under steady-state conditions, between the equation for the voltage along a TL with spatially varying properties and the convection-diffusion equation. The TL properties are directly specified by the equation to be solved and there is a rigorous method for determining the TLM model parameters from these. There is no such method for relating the CL network parameters to the CDE being solved. Instead, the relationships between the model parameters and the coefficients of the convection-diffusion equation have been established through a mixture of experiments and an analysis of the limited case where $D = 0$. While less than ideal, this has allowed the value of the scheme to be established.

The test results presented here show that the novel CL scheme can, in general, be more accurate than the VI methods (which have been shown here and previously to compare favourably with finite-difference schemes, especially when the convection term dominates). In many cases it is significantly more accurate than the VI schemes. The cost of calculating CL model parameters appears to be similar to that for the VI_C scheme but significantly lower than for the VI_{PC} scheme. The cost of calculating the steady-state equation coefficients is significantly lower than for either of the VI schemes. The CL scheme does require, however, the solution of 50% more equations. All three TLM schemes have a significant property in that their accuracy, in general, increases with increasing Peclet numbers.

The VI scheme requires current sources to model the Vdv/dx term in the CDE. The accuracy is limited by the assumption, made in deriving the equation for the node voltage, that, when considering node n, the solution between nodes $n-1$ and $n+1$ is equal to the solution at node n. The CL method, on the other hand, inherently models both convection terms in the CDE. To extend the CL scheme to model reaction terms, a similar assumption will be required. If the reaction term dominates the solution, then it is likely that the two schemes would have similar accuracy. Note that the assumption has been made for the sake of simplicity and there is no reason why more accurate formulations cannot be developed.

Systematic errors in steady-state solutions, obtained using the VI scheme, are independent of the choice of time step. This is not the case for the CL method. It would appear that, in general, the optimum value of Δt is the one for which the systematic and round-off errors have similar magnitudes. If the time step is any longer then the systematic errors may rise significantly, any lower and the round-off errors will be greater. To determine this optimum value for a given problem, the relationship between both systematic and round-off errors and Δt must be known. While a relationship between the time step and systematic errors has been established for the case where $D = 0$, further work is required to determine what effect non-zero values of D have on this relationship. Further work is also required to determine the relationship between the round-off errors and Δt.

In practice, sub-optimal values of Δt may still produce more accurate results than those obtained using other methods. Also, for some situations, as has been shown above, the errors are relatively independent of Δt over a wide range of values.

It should be noted that both schemes are equivalent to the standard 1D lossy TLM method for diffusion when $v = 0$. In the case of the VI method, the distributed capacitance and resistance are then constant over space. In the CL method, the impedance of the convection line TL segments is then infinite (i.e. $Q = 0$).

REFERENCES

1. Morton, K.W. *Numerical solution of convection-diffusion problems*. Chapman & Hall 1996
2. Majumdar, P. *Computational methods for heat and mass transfer*. Taylor & Francis Group 2005
3. Versteeg, H.K. and W. Malalasekera. *An introduction to computational fluid dynamics: The finite volume method*. Prentice Hall 1995
4. Kennedy, A. and W.J. O'Connor. A Transmission Line Modelling (TLM) method for steady-state convection-diffusion. *International Journal for Numerical Methods in Engineering* 2007. **72**(9): 1009-1028.
5. Kennedy, A. and W.J. O'Connor. A TLM method for steady-state convection-diffusion: Some additions and refinements. *International Journal for Numerical Methods in Engineering* 2009. **77**(4): 518-535
6. Pozrikidis, C. *Numerical computation in engineering and science*. Oxford University Press 1998
7. de Cogan, D. *Transmission line matrix (TLM) techniques for diffusion applications*. Gordon and Breach Science Publishers 1998
8. Johns, P.B. A simple explicit and unconditionally stable numerical routine for the solution of the diffusion equation. *International Journal of Numerical Methods in Engineering* 1977. **11**: 1307-1328.
9. Pulko, S.H. and P.B. Johns. Modeling of thermal diffusion in three dimensions by the transmission line matrix method and the incorporation of nonlinear thermal properties. *Communications in Applied Numerical Methods* 1987. **3**: 571-579.
10. de Cogan, D., W.J. O'Connor, and X. Gui. Accelerated convergence in TLM algorithms for the Laplace equation. *International Journal for Numerical Methods in Engineering* 2005. **63**: 122-138.
11. de Cogan, D. and M. Rak. Accelerated convergence in numerical simulations of surface supersaturation for crystal growth in solution under steady-state conditions. *International Journal of Numerical Modelling: Electronic Networks, Devices and Fields* 2005. **18**: 133-148.
12. O' Connor, W.J. Wave speeds for a TLM model of moving media. *International Journal of Numerical Modelling: Electronic Networks, Devices and Fields* 2002. **15**: 195-203.
13. O' Connor, W.J. TLM model of waves in moving media. *International Journal of Numerical Modelling: Electronic Networks, Devices and Fields* 2002. **15**: 205-214.
14. Kennedy, A. and W.J. O'Connor. Error analysis and reduction in lossy TLM. *International Journal for Numerical Methods in Engineering* 2008. **73**(7): 1027-1045.
15. Kennedy, A. TLM methods for convection-diffusion. *Ph.D. Thesis*, University College Dublin, 2006

x	Exact	CL	VI_C	VI_{PC}	CD	UP
0	0	0	0	0	0	0
1/3	0.0034294	0.0034287	0.0043320	0.0034523	0.0063579	−0.0062048
2/3	0.0467505	0.0467494	0.0532179	0.0468823	−0.1462307	0.1427094
1	1	1	1	1	1	1

Table 1: The exact solution at four evenly spaced nodes with $D = 1$, $v = 5 + 5x$, $V(0) = 0$, $V(1) = 1$, and equivalent results from the CL, VI, and two FD schemes.

N	6	11	21	41	81
CL	1.35E−4	3.44E−5	8.57E−6	2.15E−6	5.32E−7
VI_C	5.21E−4	1.32E−4	3.33E−5	8.33E−6	2.08E−6
VI_{PC}	9.29E−4	1.40E−4	3.48E−5	8.70E−6	2.17E−6

Table 2: The variation in the maximum errors in the solutions of models with $D = 1$, $v = 1/(1+x)$, $V(0) = 0$, and $V(1) = 1$, as measured with $\Delta t = 10^{-9}$ (CL scheme) and $\Delta t = 1$ (both VI schemes), with changes in the number of nodes, N.

v	1	2.5	5	10	20
CL	3.55E−5	1.54E−5	6.41E−5	8.32E−5	8.06E−5
VI_C	3.55E−5	5.36E−5	1.50E−4	6.45E−4	1.43E−3
VI_{PC}	7.11E−5	3.09E−5	1.28E−4	1.66E−4	1.61E−4

Table 3: The maximum errors in the solutions of models with $D = 1+x$, $V(0) = 0$, $V(1) = 1$, and 11 nodes, for different values of convection velocity.

$v(x) = 1+x$						
x	Exact Solution	Errors				
		CL	VI_C	VI_{PC}	CD	UP
0.2	8.92E−02	1.57E−07	−3.50E−04	−4.32E−05	2.39E−04	−3.17E−03
0.4	2.07E−01	2.66E−07	−6.79E−04	−8.70E−05	5.33E−04	−7.36E−03
0.6	3.72E−01	3.08E−07	−8.99E−04	−1.18E−04	8.32E−04	−1.05E−02
0.8	6.18E−01	2.38E−07	−8.17E−04	−1.07E−04	9.04E−04	−1.01E−02
$v(x) = 5+5x$						
0.2	1.18E−03	5.67E−08	−1.32E−04	−6.22E−06	1.03E−03	−2.79E−03
0.4	5.68E−03	1.06E−07	−5.14E−04	−2.35E−05	4.85E−03	−1.62E−02
0.6	2.70E−02	1.46E−07	−1.71E−03	−7.21E−05	2.17E−02	−5.19E−02
0.8	1.49E−01	1.59E−07	−4.91E−03	−1.85E−04	9.93E−02	−1.25E−01
$v(x) = 10+10x$						
0.2	2.50E−06	2.09E−10	−1.13E−06	−1.11E−08	−7.30E−04	2.94E−04
0.4	3.69E−05	3.79E−10	−1.27E−05	−9.81E−08	8.83E−03	−3.46E−03
0.6	7.46E−04	5.18E−10	−1.70E−04	−8.71E−07	−5.64E−02	−2.43E−02
0.8	2.24E−02	6.42E−10	−2.50E−03	−7.28E−06	2.89E−01	−1.31E−01

Table 4: Exact solutions for $D = 1$, $V(0) = 0$, and $V(1) = 1$, for three cases where $v(x)$ increases linearly with x, and the errors in the corresponding solutions obtained using TLM and FD schemes with 6 evenly spaced nodes.

m	1	0.98	0.95	0.9	0.8
CL	1.04E−8	3.67E−7	9.31E−7	2.05E−6	5.43E−6
VI_C	1.66E−3	1.21E−3	6.35E−4	5.64E−5	1.00E−3
VI_{PC}	7.65E−5	5.42E−5	2.31E−4	5.13E−4	1.04E−3

Table 5: The maximum errors in the solutions from models with 11 nodes and an exponential variation in node spacing, determined by the value of m.

N	11	21	41	81	161
CL	9.94E−5	3.04E−5	7.98E−6	2.03E−6	5.26E−7
VI_C	2.35E−3	6.08E−4	1.53E−4	3.84E−5	9.62E−6
VI_{PC}	8.71E−5	1.72E−5	3.99E−6	9.73E−7	2.37E−7
VI_C^*	1.56E−2	8.40E−3	4.28E−3	2.15E−3	1.07E−3
VI_{PC}^*	1.79E−2	8.99E−3	4.43E−3	2.18E−3	1.08E−3

Table 6: Differences between $V(0.5)$ as calculated by the TLM schemes and a suitable reference value calculated using the VI_{PC} scheme with exact values of dv/dx and 20001 nodes. Note that the * indicates results calculated using numerical estimates of dv/dx.

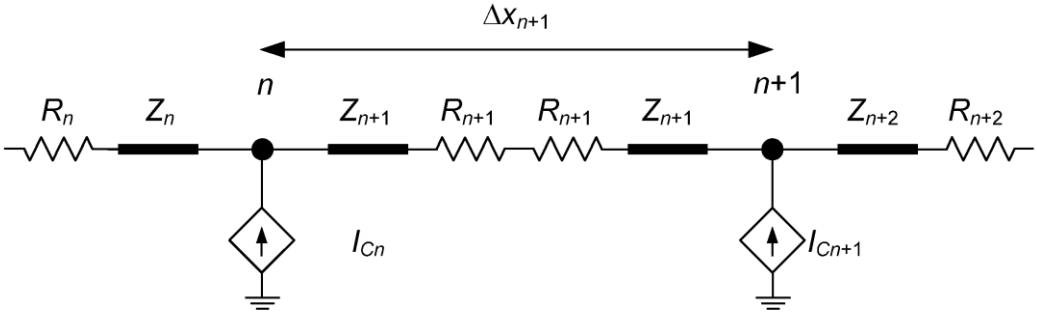

Figure 1: Two nodes, numbered *n* and *n*+1, in a TLM network. One conductor of each lossless TL segment is shown, represented by a thick line. The second conductor is connected to ground and is not shown.

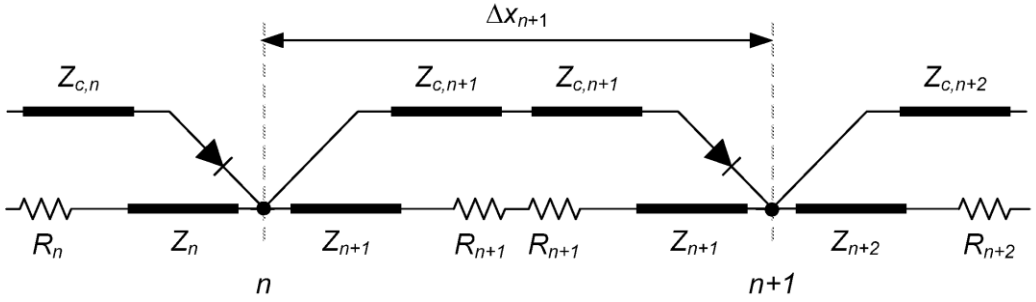

Figure 2: Two nodes, numbered *n* and *n*+1, in convection line method TLM network. The upper line, the "convection line", is connected to the lower "diffusion line" at each node.

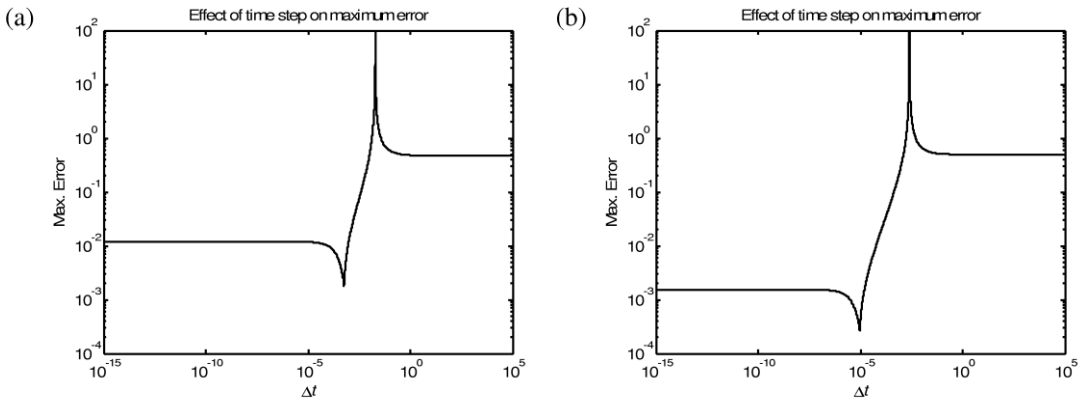

Figure 3: The variation in maximum errors with time step from models with $v(x) = 5+5x$ and $D = 0$, with (a) 11 evenly-spaced nodes and (b) 81 evenly-spaced nodes.

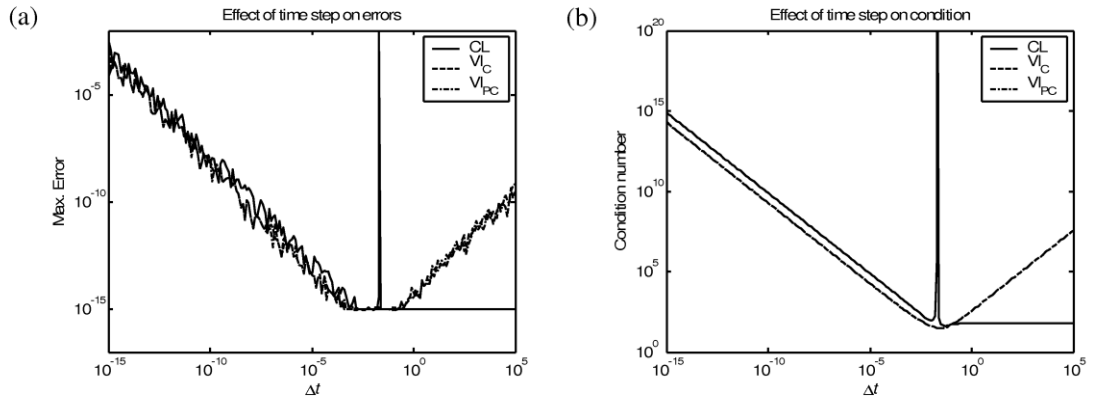

Figure 4: The maximum errors in the solutions of three models with $D = 1$, $v = 5$, $V(0) = 0$, $V(1) = 1$, and 11 evenly spaced nodes, plotted against the time step (a). Also shown are the equivalent condition numbers for the systems of steady-state equations (b). There is little difference between both the condition numbers and the maximum errors for the VI_C and VI_{PC} schemes.

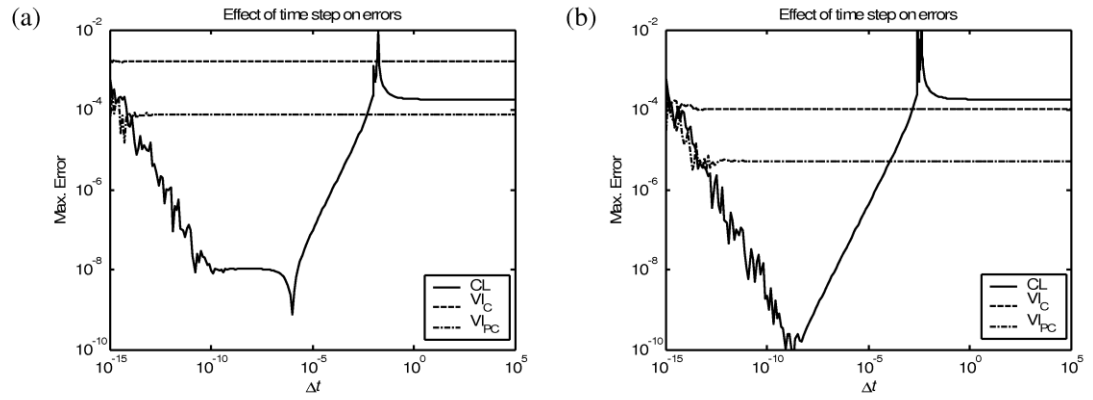

Figure 5: The maximum errors in the solutions of three models with $D = 1$, $v = 5+5x$, $V(0) = 0$, $V(1) = 1$, and 11 (a) and 41 (b) evenly spaced nodes, plotted against the time step length.